Supporting Information
B.D. Zoltowski, L.B. Motta-Mena and K.H. Gardner
"Blue-light induced dimerization of a bacterial LOV-HTH DNA-binding protein"

a.

Name	DNA sequence
	Consensus: RGNCYWWRGNCY
AN-45	GGCCCCGAGGTCCAGCACCAACGCAGT**CCCCTTTGGTAC**GCCGAC
AN-35	CGAGGTCCAGCACCAACGCAGT**CCCCTTTGGTAC**G
AN-25	TCCAGCACCAACGCAGT**CCCCTTTG**
AN-20	AGCACCAACGCAGT**CCCCTT**
AN-15	CACCAACGCAGT**CCC**
Clone-1	TCTACGTTATAGGT**AGCCTTTAGTCC**ATGCTGATTCGTTTTCAAC

b.

Name	Strand	Start	*p*-value	Sites
CLONE-3	+	2	8.42e-07	T AGACTTAAGTCT AGTACACAAG
CLONE-1	+	9	3.22e-06	TTATAGGT AGCCTTTAGTCC ATGCTGATTC
CLONE-22	+	5	8.59e-06	TATA GGGCTTTAGTCT GTATGTGGGA
CLONE-78	-	1	2.86e-05	AATAAGATAC AGTCTTAGGGCC
CLONE-53	+	19	5.79e-05	TAGTACTTAC AGTCCTTAGGCC ATG
peak-a	-	6	5.79e-05	ATCAT GGGCCAAGGTCC ATATT
peak-c	-	6	3.47e-04	TCCATAC CGCATAAAGTCT GTACC
CLONE-77	-	15	3.78e-04	CAGATAC ATGCTTTAGTAC GTATATTCGA
peak-b	-	6	4.86e-04	ACTAC CTGCTTTGGTCT AGGTC
CLONE-2	+	6	8.49e-04	AGCTA GGCTTTTGGTCT GTATAGCTGT
CLONE-74	+	11	1.40e-03	GTTATTAATC CGTATTAAGTAT GGAGGGAGAG
CLONE-55	-	8	2.35e-03	TCAGTAAACC CTTATATAGTCC TTAAGTA
an-45	+	28	3.17e-03	CCAACGCAGT CCCCTTTGGTAC GCCGAC
peak-d	+	1	3.56e-03	TGCCTTGGGCCC GCGCCGCAGC
CLONE-88	-	1	4.00e-03	CCAACAACCT GGTCATAAGGTC

Figure S1. Mapping of the canonical EL222-binding motif within the AN-45 DNA. (a) List of the DNA sequences used in the present study. The previously-identified DNA consensus sequence for EL222 [3] consists of two binding half-sites (underlined) and is shown in bold in

each of the DNA sequences. Only the forward strand is shown; R= A/G, N= any base, Y= C/T, W= A/T. **(b)** Using the sequence analysis tool MEME [4], we searched for the EL222-specific DNA motif within the AN-45 DNA and the previously identified EL222 target sequences [3]. Both the sequence logo and sequence alignment results are shown. We note that the EL222 binding site in AN-45 varies in several positions from the established consensus and the highest affinity DNA Clone-1. We predict this contributes to the ~20-fold difference in affinity between AN-45 (EC_{50}= 5-7 μM) and Clone-1 (EC_{50}= 0.3 μM).

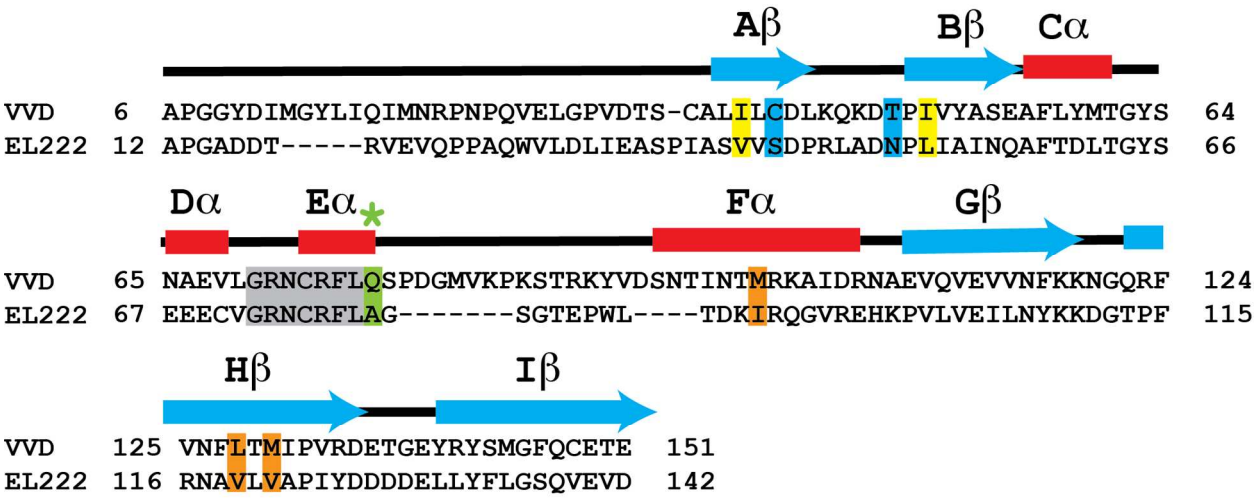

Figure S2. Sequence alignment of EL222 and VVD. Residues affecting the dark-state recovery rate in VVD [1] are highlighted; rate-accelerating (yellow) and slowing (orange) were considered for substitution. An additional residue, a conserved "Q" near the photochemically-triggered cysteine (green star), was also targeted for substitution. Residues in blue are flavin-interacting residues with negligible contributions to dark state recovery rates in other LOV proteins [1].

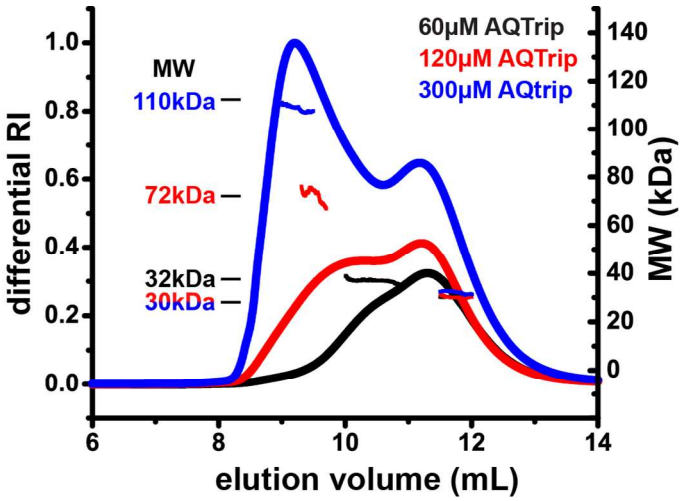

Figure S3. SEC-MALLS of light-state AQTrip reveals a concentration-dependent oligomeric state. SEC-MALLS data show that light-state AQTrip increases in MW with increasing concentration, going from a monomer at 60 μM (black) to a dimer and tetramer as concentration increased to 120 μM (red) and 300 μM (blue). MW measurements are provided from the midpoint of the MALLS traces shown.

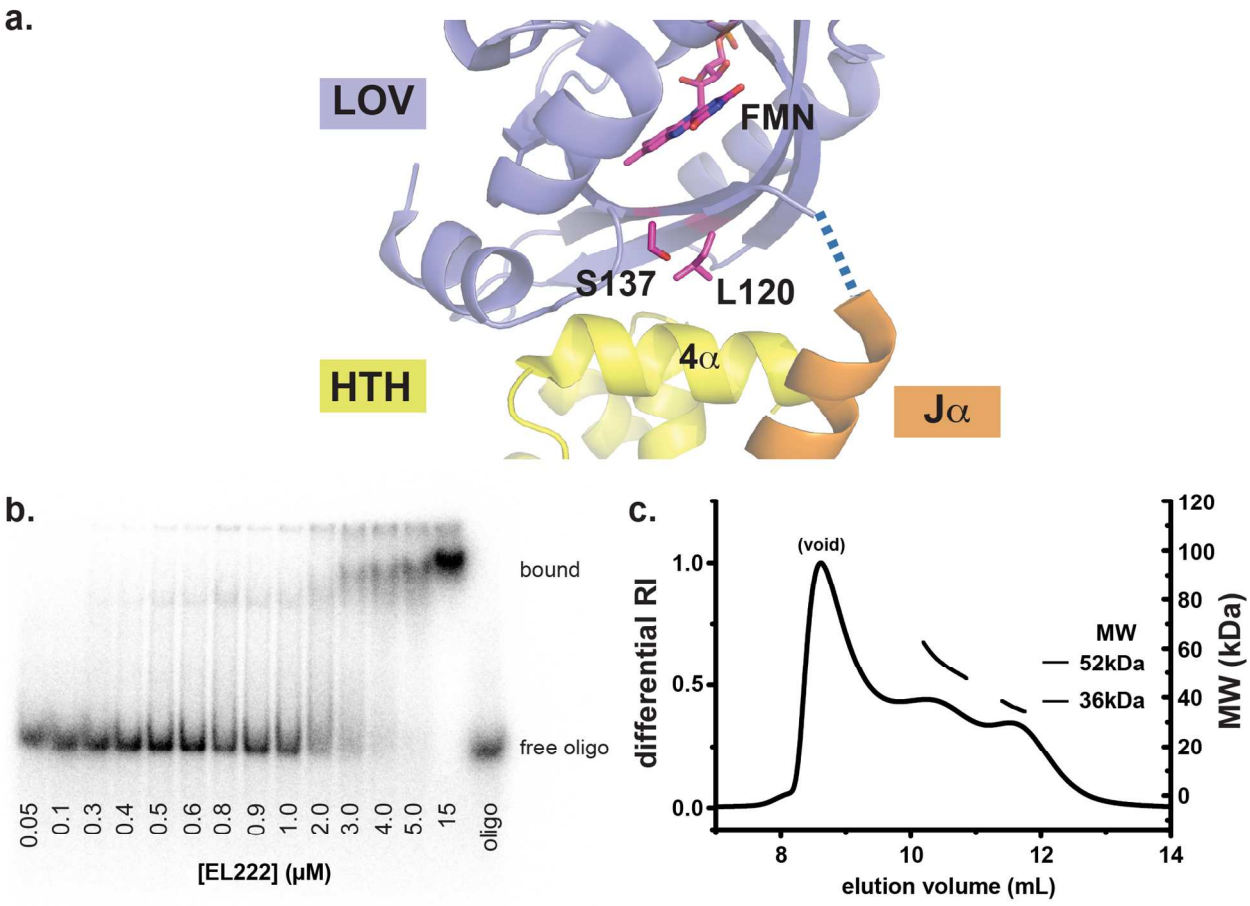

Figure S4. The S137Y LOV/HTH-disruption variant forms a protein dimer that constitutively binds DNA in the dark. (a) Both L120 and S137 lie on the LOV β-sheet, adjacent to the HTH domain 4α helix. **(b)** A dark-state EMSA of S137Y shows that the S137Y variant shifts the ^{32}P-labeled AN-45 oligo indicative of DNA-binding. Interestingly, the mutant's apparent binding affinity is slightly higher than WT EL222 (EC_{50}~2-3 μM for S137Y vs. EC_{50}~7-8 μM for WT [2]). **(c)** SEC-MALLS indicates S137Y exists as a monomer:dimer mixture at 40 μM under dark-state conditions. A large aggregate peak reflects some thermal instability in this variant (labeled as void). MW measurements are provided from the midpoint of the MALLS trace shown.

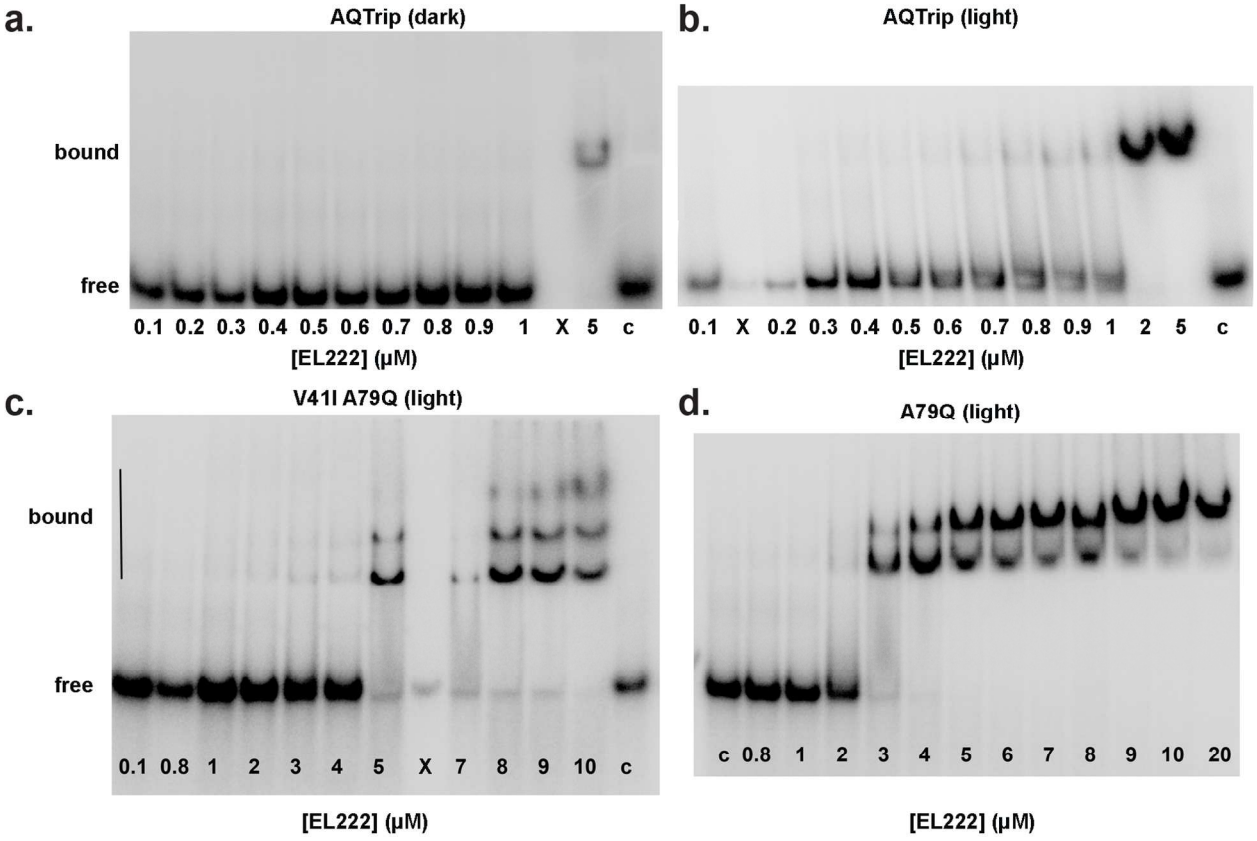

Figure S5.. EMSA analysis reveals the DNA-binding capabilities of EL222 variants. (a, b) EMSA analyses of the AQTrip variant. Dark-state samples (**a**) do not bind AN-45 DNA at or below 1 μM; however shifted bound-state bands are observed starting at ~0.7 μM under light conditions (**b**). **(c)** The V41I:A79Q variant binds DNA starting at ~2 μM under illumination, populating several bound species that suggest some additional cooperativity compared to WT. **(d)** A79Q binds DNA beginning at 2 μM, and shows fewer supershifted bands compared to V41I:A79Q. All variants elicit higher apparent binding affinities compared to WT (EC_{50}~8 μM [2]) and also have the potential to form additional higher-order protein/DNA complexes. Lanes marked with a "c" did not contain any protein; lanes marked with an "X" did not contain any DNA or protein.

References:

1. Zoltowski, B.D., B. Vaccaro, and B.R. Crane, *Mechanism-based tuning of a LOV domain photoreceptor.* Nat Chem Biol, 2009. **5**(11): p. 827-34.

2. Nash, A.I., et al., *Structural basis of photosensitivity in a bacterial light-oxygen-voltage/helix-turn-helix (LOV-HTH) DNA-binding protein.* Proc Natl Acad Sci U S A, 2011. **108**: p. 9449-9454.

3. Rivera-Cancel, G., L.B. Motta-Mena, and K.H. Gardner, *Identification of natural and artificial DNA substrates for light-activated LOV-HTH transcription factor EL222.* Biochemistry, 2012. **51**(50): p. 10024-34.

4. Bailey, T.L., et al., *MEME SUITE: tools for motif discovery and searching.* Nucleic Acids Res, 2009. **37**(Web Server issue): p. W202-8.